Journal of Naval Architecture and Marine Engineering
June, 2015
http://dx.doi.org/10.3329/jname.v12i1.12910 *http://www.banglajol.info*

FINITE ELEMENT ANALYSIS OF MAGNETO-HYDRODYNAMIC (MHD) MIXED CONVECTION FLOW IN A LID-DRIVEN TRIANGULAR CAVITY.

Mohammed Nasir Uddin[1*], Aki Farhana[2], Md. Abdul Alim[3]

[1]Dept. of Information and Communication Technology (ICT), Bangladesh University of Professionals (BUP), Mirpur-12, Dhaka-1216, Bangladesh, *Email: nasirbuet@gmail.com
[2]M. Phil students, Bangladesh University of Engineering and Technology, Dhaka-1000, Bangladesh.
[3]Department of Mathematics, Bangladesh University of Engineering and Technology, Dhaka-1000, Bangladesh.
Email: maalim@math.buet.ac.bd

Abstract:

In the present paper, the effect of magneto-hydrodynamic (MHD) on mixed convection flow within a lid-driven triangular cavity has been numerically investigated. The bottom wall of the cavity is considered as heated. Besides, the left and the inclined wall of the triangular cavity are assumed to be cool and adiabatic. The cooled wall of the cavity is moving up in the vertical direction. The developed mathematical model is governed by the coupled equations of continuity, momentum and energy to determine the fluid flow and heat transfer characteristics in the cavity as a function of Rayleigh number, Hartmann number and the cavity aspect ratio. The present numerical procedure adopted in this investigation yields consistent performance over a wide range of parameters Rayleigh number Ra (10^3-10^4), Prandtl number Pr (0.7 - 3) and Hartmann number Ha (5 - 50). The numerical results are presented in terms of stream functions, temperature profile and Nussult numbers. It is found that the streamlines, isotherms, average Nusselt number, average fluid bulk temperature and dimensionless temperature in the cavity strongly depend on the Rayleigh number, Hartmann number and Prandtl number.

***Keywords*:** MHD, mixed convection, lid-driven triangular cavity, finite element technique

Nomenclature

Gr	Grashof number	θ	dimensional temperature
Ha	Hartmann Number	*T*	temperature (K)
Re	Reynolds Number	*x, y*	Cartesian coordinates (m)
Ra	Rayleigh Number	*X, Y*	non-dimensional Cartesian coordinates
k	thermal conductivity of the fluid ($Wm^{-1}K1$)	*u, v*	velocity components (ms^{-1})
L	hight and width of the enclosure (m)		***Greek symbols***
Nu	Nusselt number	α	thermal diffusivity, ($m2s^{-1}$)
P	non-dimensional pressure	β	thermal expansion coefficient (K^{-1})
Pr	Prandtl number, υ/α	υ	kinematic viscosity of the fluid (m^2s^{-1})

1. Introduction

Many scientists, engineers and researchers studied the problems of MHD mixed convection for different types of cavity. Amongst them, Oreper and Szekely (1983) studied the effect of an externally imposed magnetic field on buoyancy driven flow in a rectangular cavity. They found that the presence of a magnetic field can suppress natural convection currents and that the strength of the magnetic field is one of the important factors in determining the quality of the crystal. Ozoe and Maruo (1987) investigated magnetic and gravitational natural convection of melted silicon two-dimensional numerical computations for the rate of heat transfer. Rudraiah et al. (1995a) investigated the effect of surface tension on buoyancy driven flow of an electrically conducting fluid in a rectangular cavity in the presence of a vertical transverse magnetic field to see how this force damps hydrodynamic movements. At the same time, Rudraiah et al. (1995b) also studied the effect of a magnetic field on free convection in a rectangular enclosure. The problem of unsteady laminar combined forced and free convection flow and heat transfer of an electrically conducting and heat generating or absorbing fluid in a

1813-8235 (Print), 2070-8998 (Online) Received: July 2013

vertical lid-driven cavity in the presence of a magnetic field was formulated by Chamkha (2002). Rahman et al. (2009a) studied the effect of a heat conducting horizontal circular cylinder on MHD mixed convection in a lid-driven cavity along with Joule Heating. The author considered the cavity of adiabatic horizontal walls and differentially heated vertical walls, but it also contains a heat conducting horizontal circular cylinder located somewhere inside the cavity. The results indicated that both the flow and thermal fields strongly depend on the size and locations of cylinder, but the thermal conductivity of the cylinder has significant effect only on the thermal field. Rahman et al. (2009b) investigated the effect on magneto-hydrodynamic (MHD) mixed convection around a heat conducting horizontal circular cylinder placed at the center of a rectangular cavity along with Joule heating. They observed that the streamlines, isotherms, average Nusselt number, average fluid temperature and dimensionless temperature at the cylinder center strongly depend on the Richardson number, Hartmann number and the cavity aspect ratio. Rahman et al. (2010) made numerical investigation on the effect of magneto hydrodynamic (MHD) mixed convection flow in a vertical lid driven square enclosure including a heat conducting horizontal circular cylinder with Joule heating. The author found that the Hartmann number, Reynolds number and Richardson number have strong influence on the streamlines and isotherms. Kumar et al.(2009) has investigated on the effects of the chemical reaction and mass transfer on MHD unsteady free convection flow past an infinite vertical plate with constant suction and heat sink. Recently, Hareesh and Narayana (2013) studied on Influence of variable permeability and radiation absorption on the heat and mass transfer in MHD micropolar flow over a vertical moving porous plate. They studied on a uniform magnetic field which acts perpendicular to the porous surface which absorbs micropolar fluid with a suction velocity varying with time. Raju et al.(2013) has shown the effect on MHD convective flow through porous medium in a horizontal channel with insulated and impermeable bottom wall. They have been obtained the expressions for flow rate, mean velocity, temperature, mean temperature, and mean mixed temperature in the flow region and the Nusselt number. Narayana and Venkataramana (2013a), investigated on the thermal radiation and heat source effects on MHD nanofluid past a vertical plate in a rotating system with porous medium and author has been discussed on the influence of various flow parameters of the flow field and explained graphically. They (2013b), also discussed on effects of Hall current and radiation absorption on MHD micro polar fluid in a rotating system. They predicted results clearly indicate that the presence of nano particles in the base fluid enhances the heat transfer process significantly. The objective of the present study is to analyze magneto-hydrodynamic (MHD) mixed convection flow in a lid-driven triangular cavity using the finite element technique.

2. Physical Model and Assumptions

The physical model considered here is shown in Fig. 1, along with the important geometric parameters. The heat transfer and the fluid flow in a two-dimensional lid-driven triangular cavity with MHD flow of which the left wall (along Y-axis) and bottom wall (along X-axis) are subjected to cold T_c and hot T_h temperatures respectively while the inclined wall is kept adiabatic. The left wall of the cavity is allowed to move upward in its own plane at a constant velocity v_0. The fluid was assumed with Prandtl number (Pr = 0.71, 1.0, 7.0) and Newtonian, and the fluid flow is considered to be laminar under magnetic field (B_0) and gravity (g). The properties of the fluid were assumed to be constant.

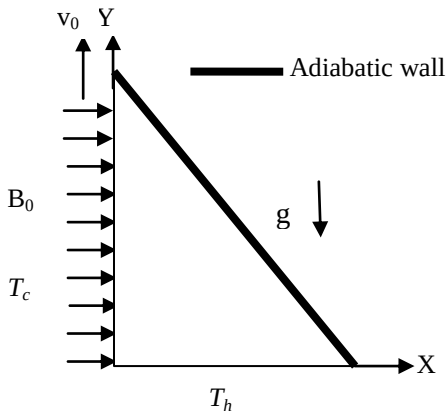

Fig. 1: Schematic diagram of the physical system

3. Mathematical Model

The fundamental laws used to solve the fluid flow and heat transfer problems are the conservation of mass (continuity equations), conservation of momentums (momentum equations), and conservation of energy (energy equations), which constitute a set of coupled, nonlinear, partial differential equations. For laminar incompressible thermal flow, the buoyancy force is included here as a body force in the *v*-momentum equation. The governing equations for the two-dimensional steady flow after invoking the Boussinesq approximation can be expressed as:

$$\frac{\partial U}{\partial X}+\frac{\partial V}{\partial Y}=0 \tag{1}$$

$$U\frac{\partial U}{\partial X}+V\frac{\partial U}{\partial Y}=-\frac{\partial P}{\partial X}+\frac{1}{Re}\left(\frac{\partial^2 U}{\partial X^2}+\frac{\partial^2 U}{\partial Y^2}\right) \tag{2}$$

$$U\frac{\partial U}{\partial X}+V\frac{\partial U}{\partial Y}=-\frac{\partial P}{\partial Y}+\frac{1}{\mathrm{Re}}\left(\frac{\partial^2 V}{\partial X^2}+\frac{\partial^2 V}{\partial Y^2}\right)+Ra\,\mathrm{Pr}\,\theta-\frac{Ha^2}{\mathrm{Re}}V \tag{3}$$

$$U\frac{\partial \theta}{\partial X}+V\frac{\partial \theta}{\partial Y}=\frac{1}{Re\,Pr}\left(\frac{\partial^2 \theta}{\partial X^2}+\frac{\partial^2 \theta}{\partial Y^2}\right) \tag{4}$$

With the boundary conditions

The dimensionless boundary conditions under consideration can be written as:

At the vertical wall: U = 0, V= 1, $\theta=0$

At the horizontal wall: U = 0 , V= 0, $\theta=1$

At the inclined wall: U = 0, V= 0, $\frac{\partial\theta}{\partial N}=0$

Where *N* is the non-dimensional distances either along *X* or *Y* direction acting normal to the surface and *K* is the dimensionless thermal conductivity. The average Nusselt number at the heated wall of the cavity based on the non-dimensional variables may be expressed as $Nu=-\int_0^1\left(\frac{\partial\theta}{\partial Y}\right)_{y=0}dX$ and the bulk average temperature defined as $\theta_{av}=\int\theta\,d\overline{V}/\overline{V}$, where $\overline{V}$ is the cavity volume.

The above equations were normalized using the following dimensionless scales:

$$X=\frac{x}{L},Y=\frac{y}{L},U=\frac{u}{U_0}\;V=\frac{v}{V_0},\;\mathrm{Pr}=\frac{\nu}{\alpha}\;\mathrm{Re}=\frac{u_i L}{\nu},\;\mathrm{Pr}=\frac{\nu}{\alpha},\;Gr=\frac{\beta g\Delta T L^3}{\nu^2},\;Ha^2=\frac{\sigma B_0^2 L^2}{\mu}$$

$$\Delta T=T_h-T_c,\alpha=\frac{\kappa}{\rho C_p}$$

4. Numerical Analysis

The governing equations along with the boundary conditions are solved numerically by employing Galerking weighted residual finite techniques. The application of this technique is well described by Zienkiewicz and Taylor (1991) and Dechaumphai (1999). The finite element formulation and computational procedure are omitted herein for brevity.

5. Grid Independence Test

Test for the accuracy of grid fineness has been carried out to find out the optimum grid number. In order to obtain grid independent solution, a grid refinement study is performed for a square open cavity with *Pr* = 0.71, *Re*= 50 and *Ra* = 10^4. Fig. 2 shows the convergence of the average Nusselt number, Nu_{av} at the heated surface with grid refinement. It is observed that grid independence is achieved with 13398 elements where there is insignificant change in Nu with further increase of mesh elements. Six different non-uniform grids with the following number of nodes and elements were considered for the grid refinement tests: 11616 nodes, 1936 elements; 23256 nodes, 3876 elements; 30162 nodes, 5027 elements; 45330 nodes, 7555 elements; 65514 nodes, 10919 elements; 80388 nodes, 13398 elements, 97716 nodes, 16286 elements. From these values, 80388 nodes, 13398 elements can be chosen throughout the simulation to optimize the relation between the accuracy required and the computing time as shown in Table 1.

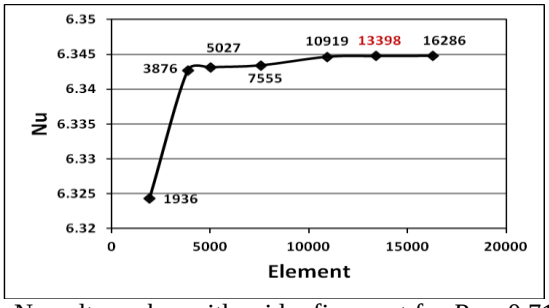

Fig. 2: Convergence of average Nusselt number with grid refinement for *Pr* = 0.71, *Re*= 50, *Ha*=20 and *Ra* = 10^4.

Table 1: Grid Sensitivity Check at *Pr* = 0.71, *Re*= 50, *Ha*=20 *and Ra* = 10^4.

Nodes (elements)	11616 (1936)	23256 (3876)	45330 (7555)	65514 (10919)	80388 (13398)	97716 (16286)
Nu	6.3243	6.3426	6.3434	6.3446	6.3447	6.3447
Time (s)	15.422	30.562	63.312	118.578	159.563	190.016

6. Results and Discussion

The MHD mixed convection flow and temperature fields as well as heat transfer rates and bulk temperature inside the lid-driven triangular cavity has been numerically investigated.

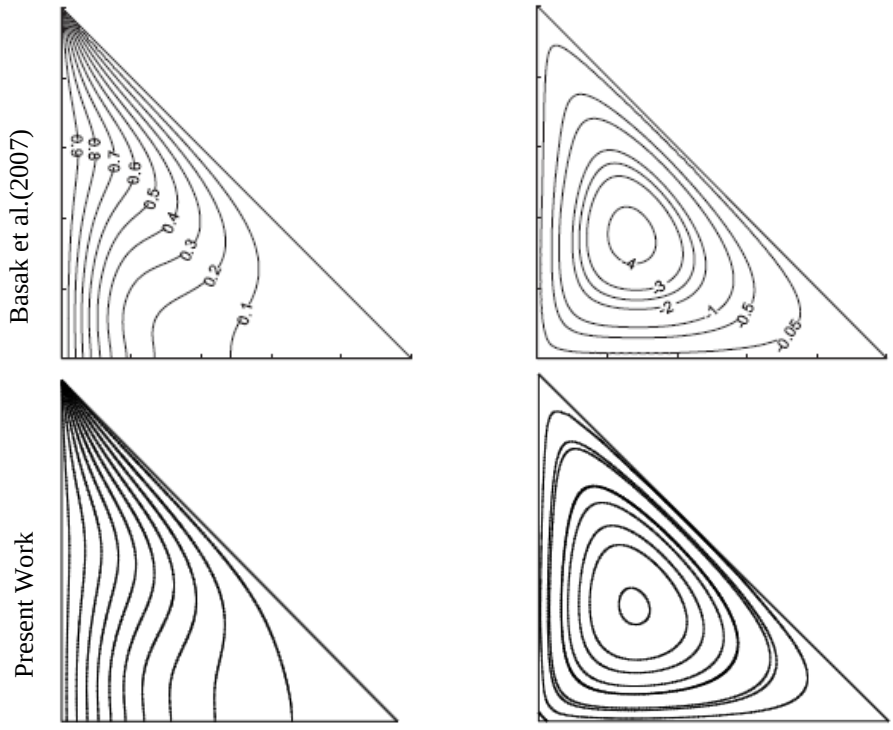

Isotherms Streamlines

Fig. 3: Comparison of the results for the constant surface temperature with Pr = 0.71.

The MHD mixed convection phenomenon inside the enclosure is strongly influenced by governing as well as physical parameters, namely and Hartman number *Ha*, Reynolds number *Re*, Prandtl number *Pr*, Rayleigh number *Ra*. As the nature of flow and thermo physical properties of fluid strongly influenced on the heat transfer rate, and the numerical computation were performed for a range of *Ha* (0.0-50), *Re* (40-100) and *Pr* (0.71-6). In addition, for each value of mentioned parameters, computations are performed at *Ra* $=5\times10^3$ that

focuses on pure mixed convection. Moreover, the results of this study are presented in terms of streamlines and isotherms. Furthermore, the heat transfer effectiveness of the enclosure is displayed in terms of average Nusselt number *Nu* and the dimensionless average bulk temperature. In Fig. 3, a comparison with Basak et al. (2007) for the average Nusselt numbers is presented.

6.1 Effects of Reynolds number (Re)

The effects of Reynolds number on the flow structure and temperature distribution are depicted in Figs. 4 and 5. The streamlines are presented for different values of Rayleigh numbers (Ra), Reynolds numbers (Re) ranging from 10^3 to 10^4 and 40 to 100 respectively while *Pr* = 0.71, and *Ha* =20. Now at *Re* = 40, the fluid near to the hot (bottom) wall has lower density, so it moves upward while the relatively heavy fluid near to cold (left) wall and this fluid is heated up. Thus the fluid motion completes the circulation. A very small value of contour rotating cell is observed in the middle part of the cavity as primary vortex. The secondary vortex cell is shown around the primary vortex in the cavity. The secondary vortex are more packed to the respective wall dramatically for the increasing value of *Re* that implies the flow moves faster and the velocity boundary layer become thinner. Moreover, it is clearly seen that the center vortex become bigger with increasing *Re* due to conduction intensified gradually. The value of the magnitudes of the stream function is greater due to mechanically driven circulations.

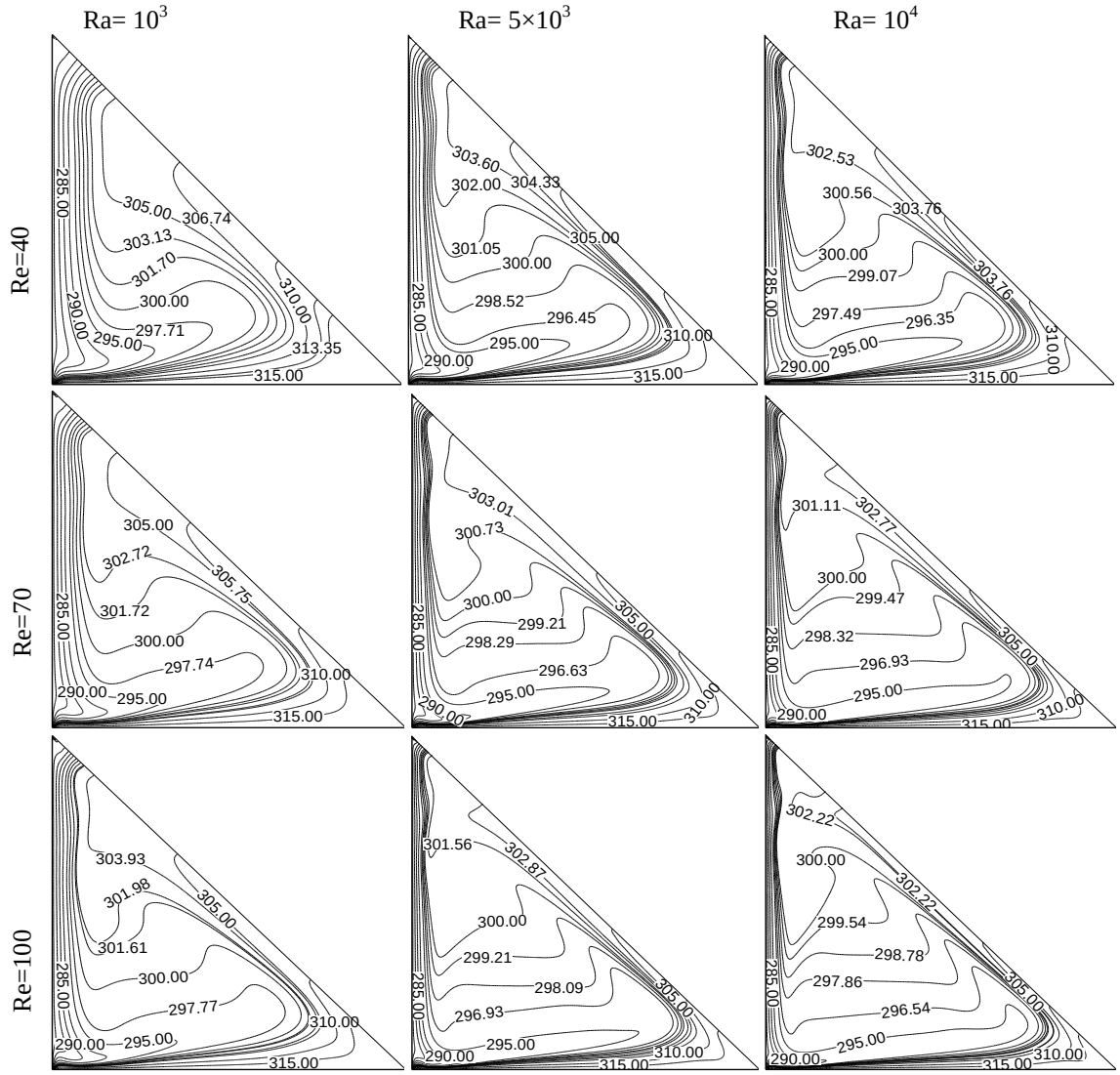

Fig. 4: Isotherms patterns for different Re (40, 70, 100) when Pr = 0.71 and Ha=20

The corresponding isotherm pattern for different value of Reynolds number while *Pr* = 0.71 and *Ha*=20 is shown in Fig. 4. From this figure, it is found that the isotherms are more congested at the heated wall of the cavity testifying the noticeable increase in convective heat exchange. The temperature gradients are very small due to mechanically driven circulations at the left wall of the cavity. It is also noticed that the thermal boundary layer near the heated wall becomes thinner with increasing *Re.* Due to high circulations, the temperature contours condensed in a very small regime at the upper portion of the left wall and this may cause greater heat transfer rates at the heated wall.

The effects of Reynolds number on average Nusselt number *Nu* at the heated wall and the average bulk temperature θ_{av} of the fluid in the cavity are illustrated in Figs. 6 and 7, while *Pr* = 0.71, *Ha* = 20. From Fig. 6, it is seen that the average Nusselt number *Nu* increases steadily with increasing Rayleigh number. This arises from the fact that physical properties of fluid changes to better heat transfer. For *Re* = 100, it is noticed that the average Nusselt number *Nu* increases sharply but increase of *Nu* befall slower for lower value of *Re* (= 40).
Fig. 7 displays the variation of the average bulk temperature against the Rayleigh number for various Reynolds numbers. The average temperature decreases smoothly with increase of Ra. It is an interesting observation that at lower *Re*, the average bulk temperature is affected by Rayleigh number.

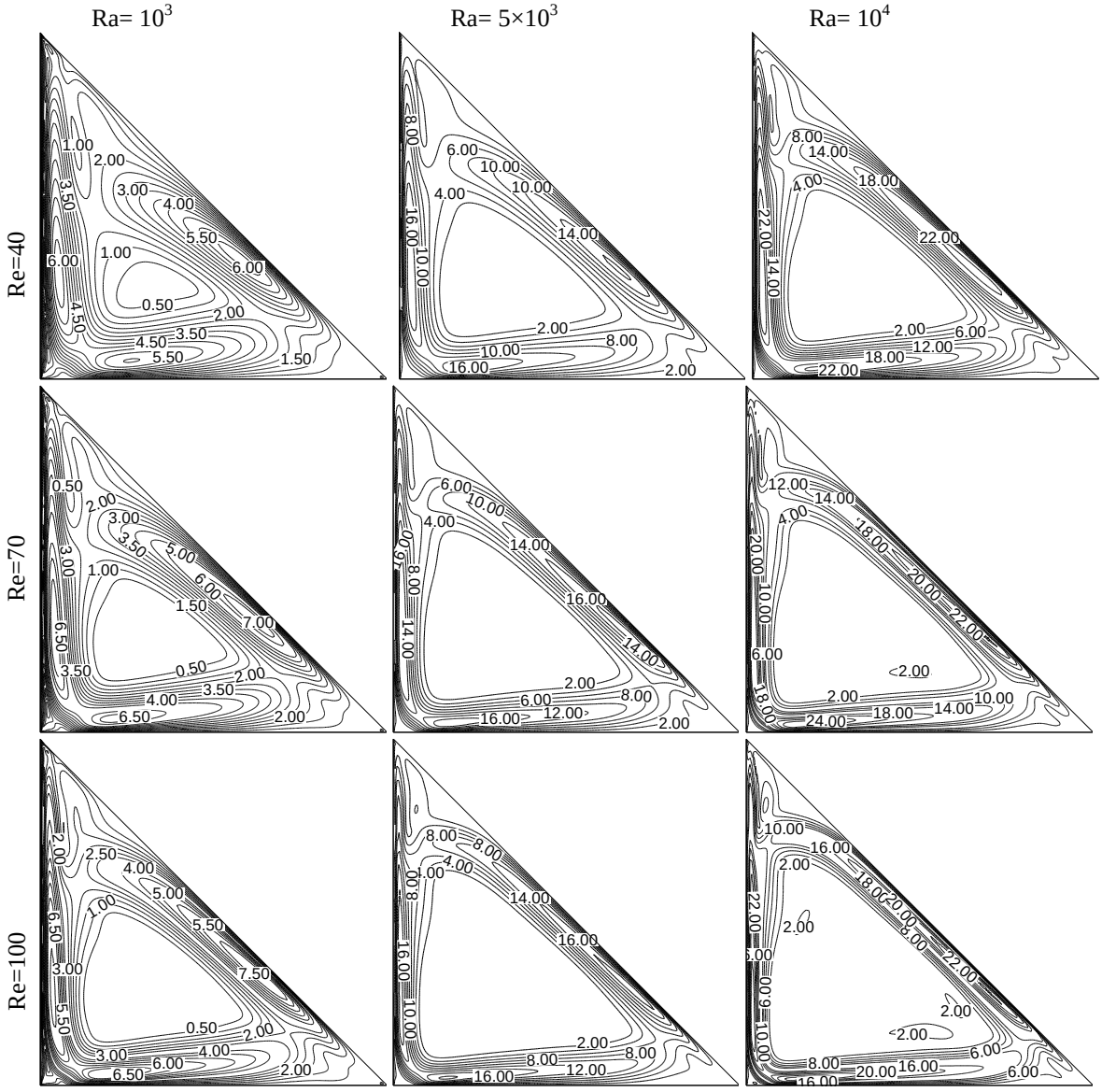

Fig. 5: Streamlines patterns for different Re (20, 70,100) when *Pr* = 0.71and *Ha=20*

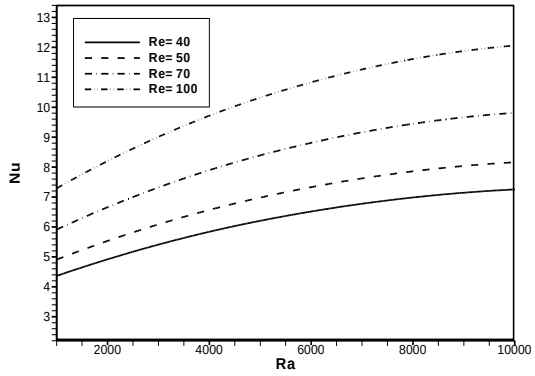

Fig. 6: Effect of average Nusselt number and Rayleigh number while Pr = 0.71, Ha = 20.

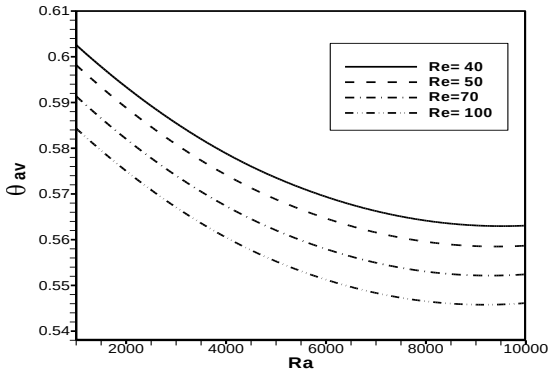

Fig. 7: Effect of average bulk temperature and Rayleigh number while *Pr* = 0.71, *Ha* = 20.

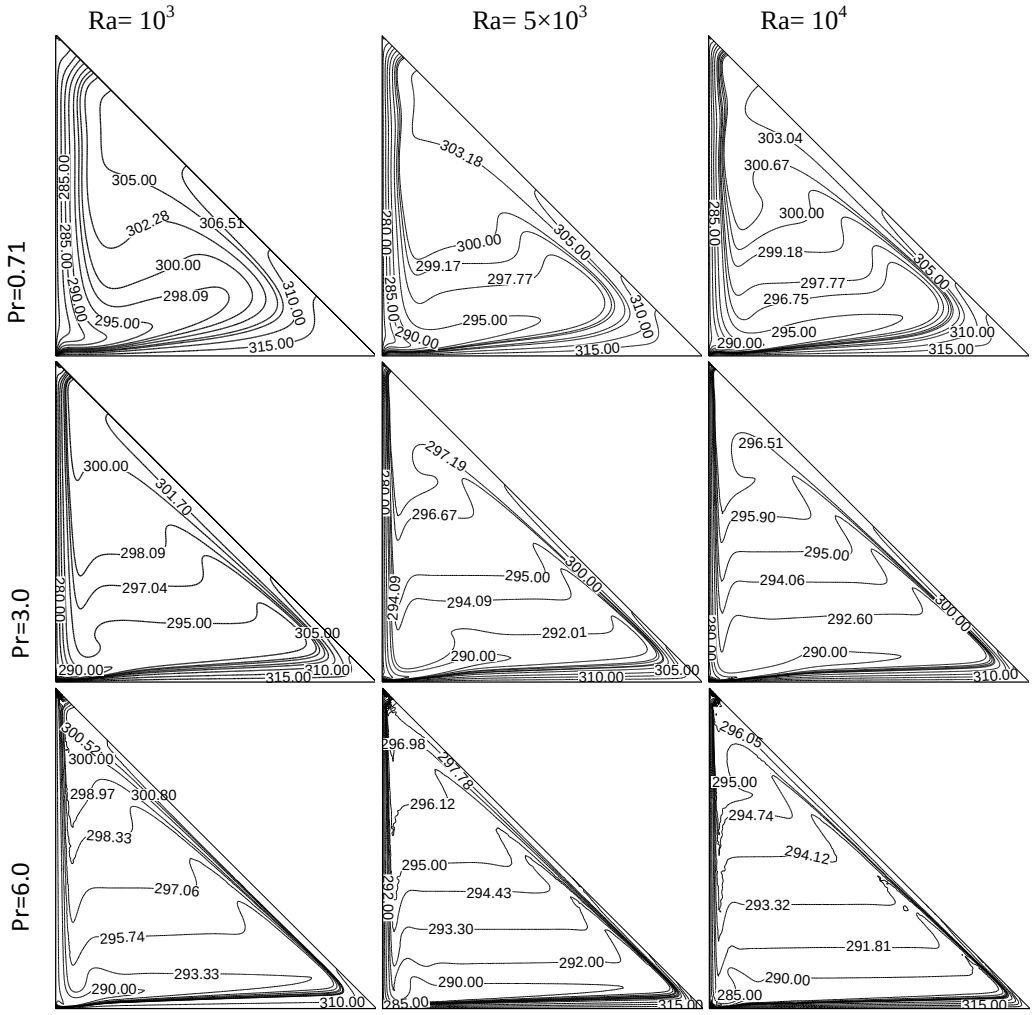

Fig. 8: Isotherms patterns for different Pr (0.71, 3.0, 6.0) when Re = 50 and Ha=20

6.2 Effect of Prandtl number (*Pr*)

The property of Prandtl number on flow fields for the considered *Ra* is depicted in Figs. 8 and 9, while *Re* = 50 and Ha=20 are kept fixed. Now, from the figure it seen that a small vortex is formed at the center of the cavity. It is evident that the size of the vortex is increased with the increasing value of *Pr*. The thermal boundary layer decreases in thickness as *Pr* increases. This is reflected by the denser deserting of isotherms close to the heated wall and cooled wall as *Pr* increases. The spread of isotherms at low values of *Pr* is due to a strong stream wise

conduction that decreases the stream wise temperature gradient in the field. At the increase of *Pr* the isotherms become linear in the cavity and impenetrable to respective wall. From Fig. 8, it can easily be seen that the isotherms for different values of *Pr* at $Ra = 10^4$ are clustered near the heated horizontal wall and cooled vertical heated surface of the enclosure, indicating steep temperature gradient along the vertical direction in this region. Besides, the thermal layer near the heated wall becomes thinner moderately with increasing *Pr*.

The effects of Prandtl number on average Nusselt number *Nu* at the heated surface and average bulk temperature θ_{av} in the cavity is illustrated in Figs. 10 and 11 with *Re* =50 and Ha=20. From this figure, it is found that the average Nusselt number *Nu* goes up penetratingly with increasing *Pr*. It is to be highlighted that the highest heat transfer rate occurs for the highest values of *Pr* (= 6). The average bulk temperature of the fluid in the cavity declines very mildly for higher values of *Pr* (0.71- 6.0). But for the lower values of *Pr*, the average bulk temperature is linear. It is to be mentioned here that the highest average temperature is documented for the lower value of *Pr* (=0.71) in the free convection dominated region.

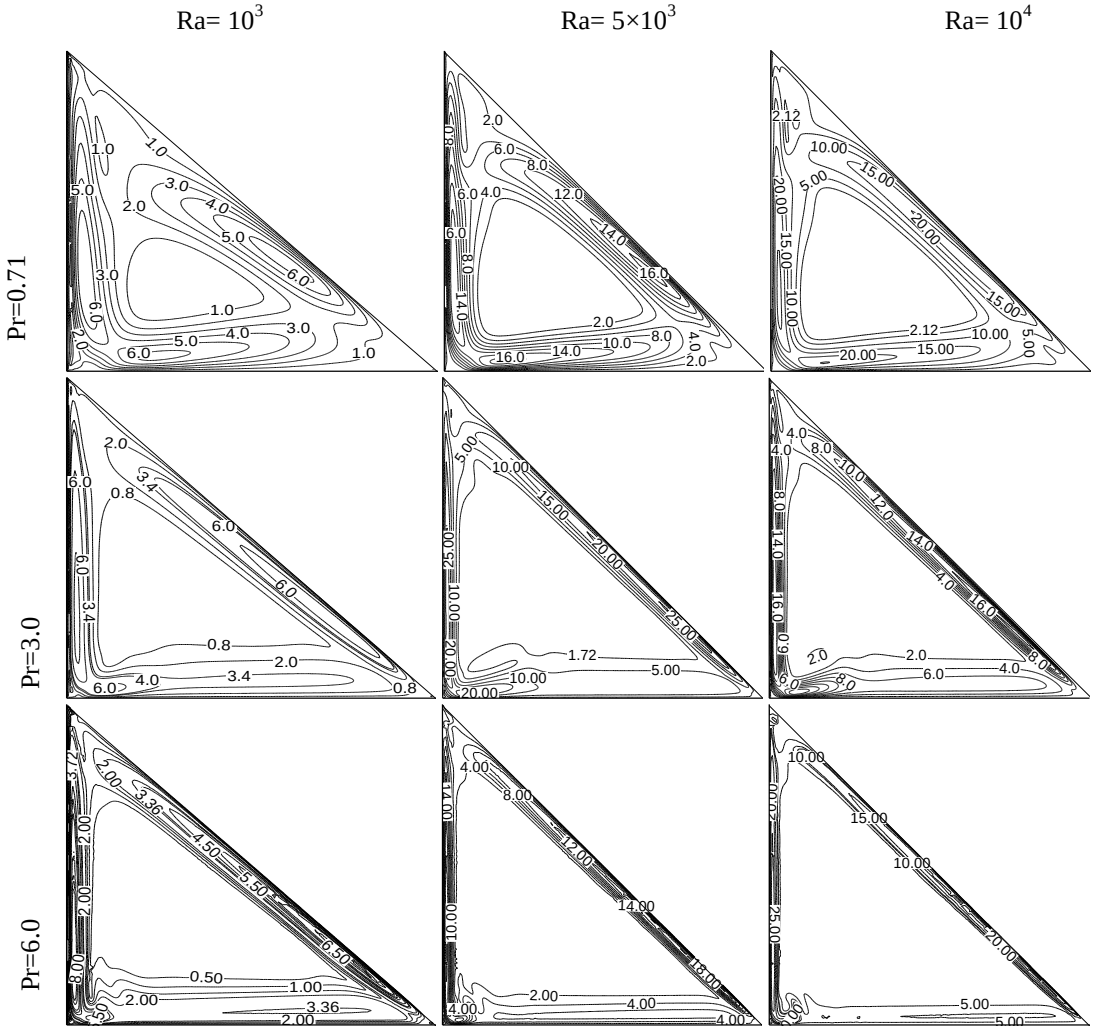

Fig. 9: Streamline patterns for different Pr *(0.71, 3.0, 6.0) when Re* = 50 and *Ha=20*

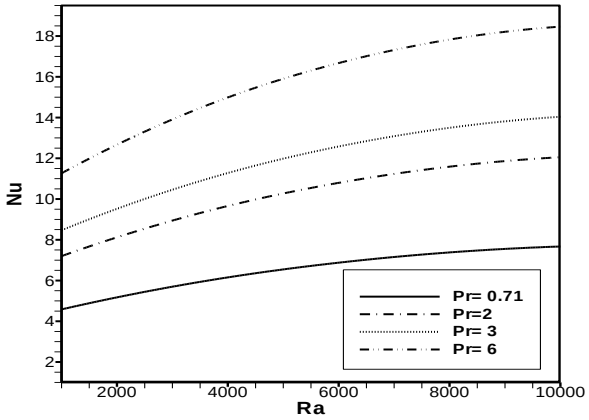

Fig. 10: Effect of average Nusselt number and Rayleigh number while Re = 50 and Ha=20

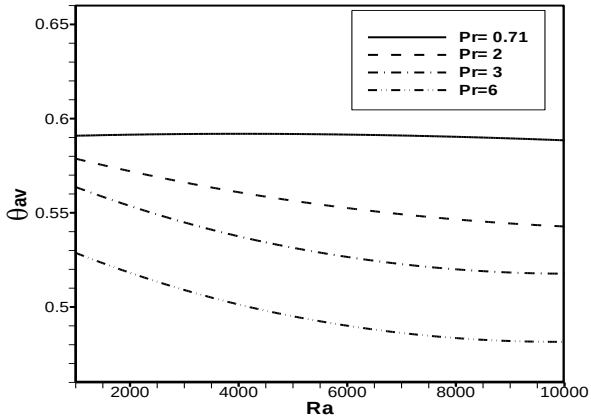

Fig. 11: Effect of average bulk temperature and Rayleigh number while Re = 50 and Ha=20.

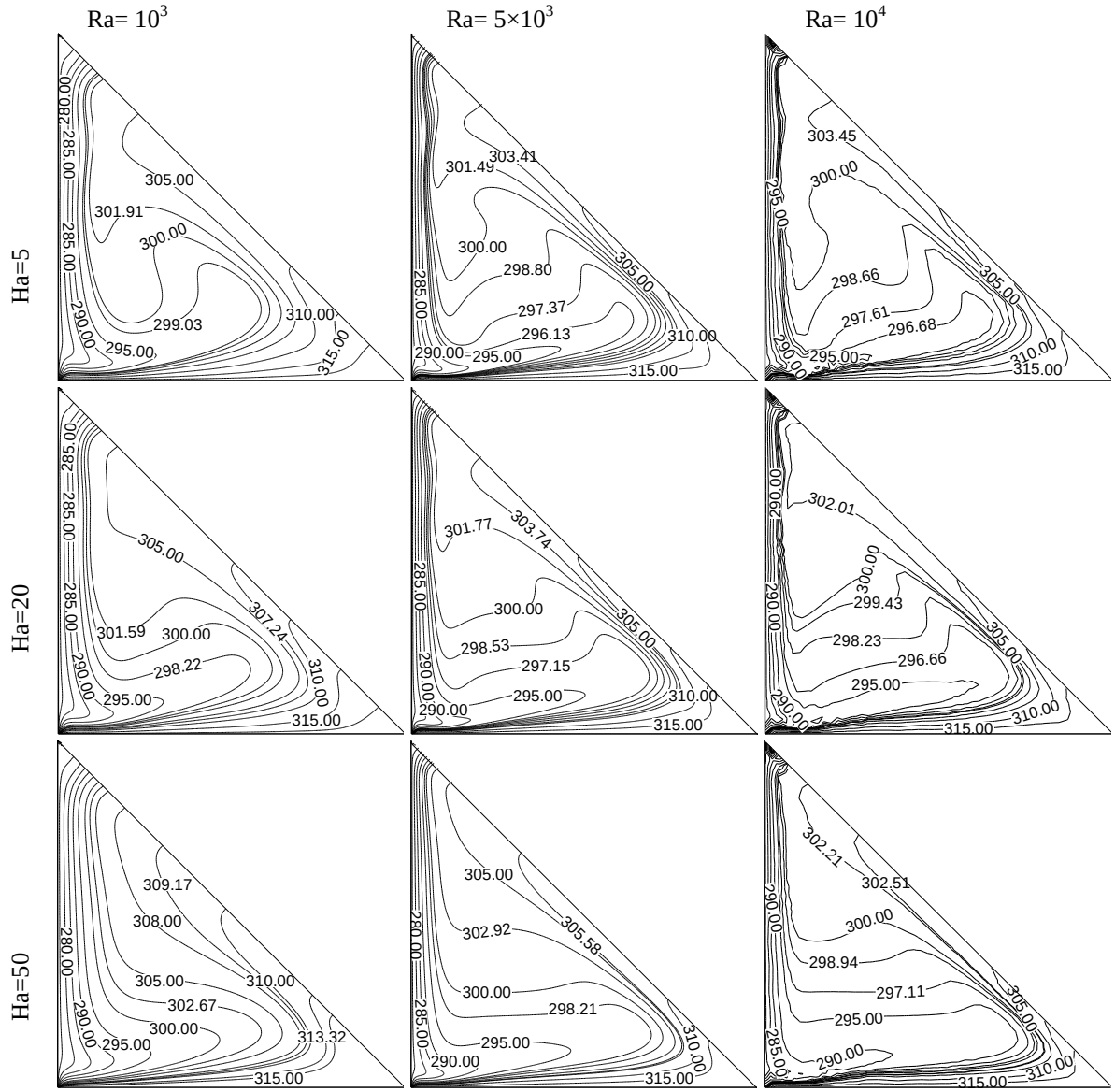

Fig. 12: Isotherm patterns for different *Ha (00, 20.0, 50.0) when Re* = 50 and *Ra*= 10^3

6.3 Effects of Hartmann number

The special effects of Hartmann number *Ha* on the flow and thermal fields at $Ra = 1e^3$ to $1e^4$ is illustrate in Figs. 12 and 13, while $Pr = 0.71$ and $Re = 50$ are kept fixed. In this folder, the size of the counter clockwise vortex also decreases sharply with increasing of *Ha*. This is because application of a slanting magnetic field has the propensity to slow down the movement of the buoyancy induced flow in the cavity. The effects of Hartmann number *Ha* on isotherms are shown in the Fig. 12 while $Re = 50$ and $Pr = 0.71$ are kept fixed. It is observed that the higher values isotherms are more tightened at the vicinity of the heated wall of the cavity for the considered value of *Ra*. A similar trend is found for the higher values of *Ha*. From this figure it can easily be seen that isotherms are almost parallel at the vicinity of the bottom horizontal hot wall but it changes to parabolic shape with the increasing distance from inclined wall for the highest value of *Ha* (=20.0) at Pr=0.71, indicating that most of the heat transfer process is carried out by conduction. In addition, it is noticed that the isothermal layer near the heated surface becomes slightly thin with the decreasing *Ha*. However in the remaining area near the left wall of the cavity, the temperature gradients are small in order to mechanically driven circulations.

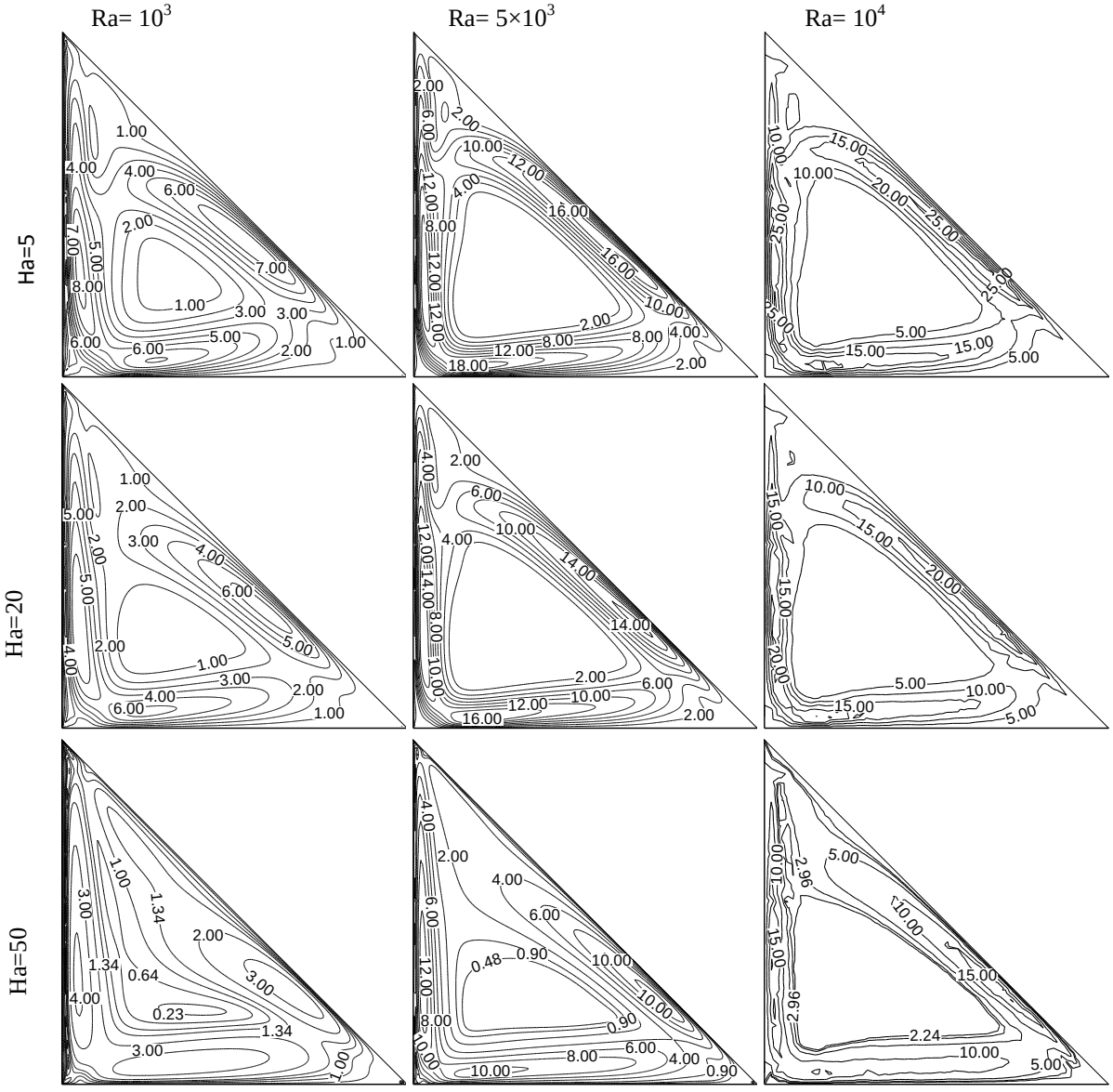

Fig. 13: Stream line patterns for different *Ha (00, 20.0, 50.0) when Re* = 50 and $Ra=10^3$

The effects of *Ha* on average Nusselt number *Nu* at the heated surface and average bulk temperatureθ_{av} in the cavity is illustrated in Figs.14 and 15 with *Re* =50 and *Pr* =0.71. From this figure, it is found that the average Nusselt number *Nu* decreases with increasing *Pr*. It is to be highlighted that the highest heat transfer rate occurs for the lowest values of *Ha* (= 5). The average bulk temperature of the fluid in the cavity is high for higher values of *Ha* (10-50). It is to be mentioned here that the highest average temperature is documented for the higher value of *Ha* in the free convection dominated region.

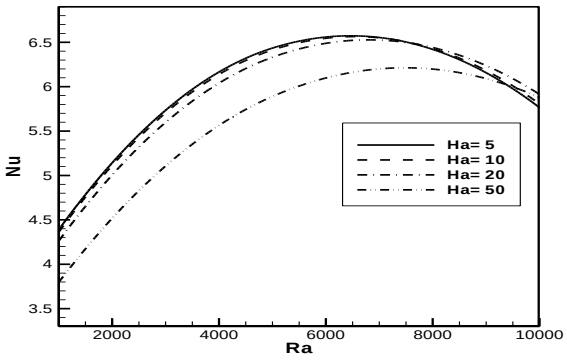

Fig. 14: Effect of average Nusselt number and Rayleigh number while *Pr* = 0.71 and *Re* = 50.

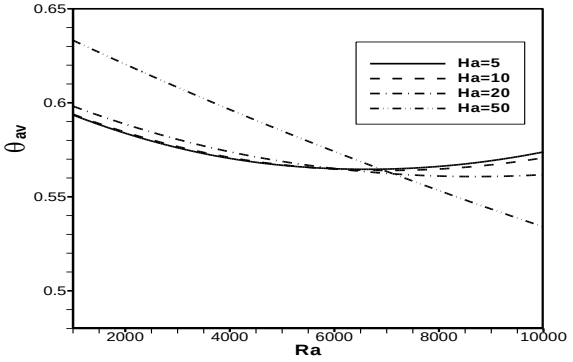

Fig. 15: Effect of average bulk temperature and Rayleigh number while *Pr* = 0.71and *Re* = 50

7. Conclusion

A two dimensional, steady combined convection flow with MHD effect in the triangular cavity has been studied and subjected to cool at the left vertical wall which is moving, adiabatic conditions at the other inclined wall and the bottom wall considered as heated. The finite element equations were derived from the governing flow equations that consist of the conservation of mass, momentum, and energy equations. The derived finite element equations are nonlinear requiring an iterative technique. The Galerking weighted residual method is applied to solve these nonlinear equations for solution to the nodal velocity components, temperatures, and pressures. The above example demonstrates the capability of the finite element formulation that can provide insight to steady-state incompressible conjugate effect of mixed convection and conduction problem. The major outcomes have been summarized as below:

- The magneto-hydrodynamic (MHD) has significant effect on the flow and thermal distributions in the triangular cavity. The average Nusselt number (*Nu*) at the hot wall is the highest for the *Pr* = 6.0 when Rayleigh number 10^4, whereas the lowest heat transfer rate for the *Ha* = 50 when Rayleigh number 10^3. Moreover, the average Nusselt number with MHD effect is considered higher than those obtained without MHD effect for different value of *Pr* number. However, the average bulk temperature at the hot wall is the lowest for the *Pr* = 6.0 when Rayleigh number 10^4, whereas the highest rate for the *Ha* = 50 when Rayleigh number 10^3
- The heat transfer rate increase steadily with the increase of *Ra*. Increasing *Ra* refers that the fluid flow switches from conductive to convective heat transfer. The bulk Temperature decreases smoothly with the increase of *Ra* because at constant conductivity bulk temperature is inversely proportional to the *Nu* (Average Heat Transfer rate).
- The heat transfers rate augment with the increase of *Ra* because when *Pr* number increases, the convective heat transfer dominated inside the flow field. The bulk Temperature remain linear at *Pr* = 0.71 because for low *Pr* number conduction heat transfer dominate in the cavity. But for higher *Pr* bulk temperature decreases due to conduction turn into convection.
- With the increase of *Ha* number electromagnetic conduction increases that slow down the heat transfer rate though it increases at forced convection dominated region for a while but fall steadily in mixed convection dominated region.
- Thermal boundary layer thickness is thinner and velocity of fluid flow increases for increasing of Rayleigh number due to convective heat transfer.
- Various vortices inflowing into the flow field and secondary vortex at different place in the cavity.

References

Basak, T., Roy, S. and Thirumalesha, C. (2007): Finite Element Analysis of Natural Convection in a Triangular Enclosure: Effects of Various Thermal Boundary Conditions, Chemical Engineering Science, Vol. 62, No.9, pp. 2623– 2640.

Chamkha, A. J. (2002): Hydro-Magnetic Combined Convection Flow in a Vertical Lid-Driven Cavity With Internal Heat Generation or Absorption, Numerical Heat Transfer, Part A, Vol. 41, No.5, pp. 529-546.

Dechaumphai, P. (1999): Finite Element Method in Engineering, Second Ed., Chulalongkorn University Press, Bangkok.

Babu, H. D. and Narayana, P.V. S. (2013): Influence of Variable Permeability and Radiation Absorption on the Heat and Mass Transfer in MHD Micropolar Flow Over a Vertical Moving Porous Plate, ISRN Thermodynamics, Vol. 2013, pp.1-17. http://dx.doi.org/10.1155/2013/953536.

Kumar, J. G., Narayana, P.V. S. and Ramakrishna, S. (2009): Effects of The Chemical Reaction and Mass Transfer on MHD Unsteady Free Convection Flow Past an Infinite Vertical Plate With Constant Suction and Heat Sink, Ultra Science, Vol. 21, No. 3, pp.639-650.

Narayana, P. V. S., Venkateswarlu, B. and Venkataramana, S.V. (2013a): Effects of Hall Current and Radiation Absorption on MHD Micropolar Fluid in a Rotating System, Ain Shams Engineering Journal,Vol.4, No.4, pp.843-854.

Narayana , P.V. S., Venkateswarlu, B. and Venkataramana, S.V. (2013b): Thermal Radiation and Heat Source Effects on MHD Nanofluid Past a Vertical Plate in A Rotating System With Porous Medium, Heat Transfer-Asian Research, Vol. 44, No.1, pp. 1-19. http://dx.doi.org/10.1002/htj.21101.

Oreper, G. M. and Szekely, J.(1983): The Effect of an Externally Imposed Magnetic Field on Buoyancy Driven Flow in a Rectangular Cavity, Journal of Crystal Growth, Vol. 64, No.3, pp. 505-515.

Ozoe, H., and Maruo, M.,(1987): Magnetic and Gravitational Natural Convection of Melted Silicon-Two Dimensional Numerical Computations for The Rate of Heat Transfer, JSME, Vol. 30, No.363, pp. 774-784.

Raju, K.V.S., Reddy, T. S., Raju, M.C. and Narayana, P.V. S. and Venkataramana, S.V. (2013): MHD Convective Flow Through Porous Medium in a Horizontal Channel With Insulated and Impermeable Bottom Wall in The Presenceof Viscous Dissipation and Joule Heating, Ain Shams Engineering Journal, Vol.5, No.1, pp. 543-551. http://dx.doi.org/10.1016/j.asej.2013.10.007

Rahman, M. M., Alim, M. A., Mamun, M. A. H., Saidur, R. and Nagata, S. (2009a): Effect Of a Heat Conducting Horizontal Circular Cylinder on MHD Mixed Convection in a Lid- Driven Cavity Along With Joule Heating, International Journal of Mechanical and Materials Engineering (IJMME), Vol. 4, No. 3, pp.256-265.

Rahman, M. M., Alim, M. A. and Chowdhury, M. K. (2009b): Magneto-hydrodynamic Mixed Convection Around A Heat Conducting Horizontal Circular Cylinder in a Rectangular Lid-Driven Cavity With Joule Heating, Journal of Scientific Research, Vol.1, No.3, pp.461-472.

Rahman, M. M. and Alim, M. A. (2010): MHD Mixed Convection Flow in a Vertical Lid-Driven Square Enclosure Including a Heat Conducting Horizontal Circular Cylinder with Joule Heating, Nonlinear Analysis: Modeling and Control, Vol. 15, No. 2, pp.199-211.

Rudraiah, N., Venkataachalaaappa, M. and Subbaraya, C. K. (1995a): Combined Surface Tension and Buoyancy-Driven Convection In A Rectangular Open Cavity In The Presence Of Magnetic Field International Journal Non-linear Mechanics, Vol. 30, No.5, pp. 759-770.

Rudraiah, N., Venkataachalaaappa, M. and Subbaraya, C. K. (1995b): Effect of Magnetic Field on Free Convection in a Rectangular Enclosure, International Journal of Engineering Science, Vol. 33, No.8,pp. 1075-1084.

Zienkiewicz, O. C. and Taylor, R. L. (1991): The Finite Element Method, Fourth Ed., McGraw-Hill.